Picosecond and Sub-Picosecond Flat-Top Pulse Shaping Using Abrupt Taper Interferometers

Changjian Guo, *Student Member, IEEE*, Michael Nix, Scott S.-H. Yam, *Member, IEEE*, and Sailing He, *Senior Member, IEEE, Fellow, OSA*

***Abstract*—A picosecond flat-top pulse shaper using an abrupt taper interferometer is proposed and experimentally demonstrated. A theoretical model based on coupled mode equations is also derived to simulate the propagation of picosecond pulses through the abrupt taper interferometer. Through properly designing the abrupt taper interferometer, a 3.8-ps flat-top pulse with less than 4% ripple is successfully generated from a 2.2-ps Gaussian pulse. The proposed technique can also be used in the sub-picosecond regime.**

***Index Terms*—Abrupt taper interferometer, flat-top pulse generation, pulse shaping.**

I. Introduction

TECHNIQUES for manipulating the temporal shape of ultra short pulses with pulse widths in the picosecond and sub-picosecond regimes have attracted much research interest, since they play an important role in ultra-high speed communications [1]–[6]. In particular, picosecond and sub-picosecond flat-top pulses are used intensively in high speed optical switching and demultiplexing applications to improve the timing jitter tolerance [3], [5], [6] and to avoid pulse break up [1].

Various methods have been reported to generate flat-top pulses [7]–[14]. Among these techniques, the most commonly used is Fourier domain pulse shaping [7]–[9], in which the frequency components of an input pulse are dispersed and their amplitudes and phases are manipulated in order to obtain the required pulse shape. Although this technique can provide significant flexibility in synthesizing arbitrary waveforms, its requirement for bulk-optics devices (diffraction gratings, phase masks, liquid-crystal spatial light modulators (LCMs), acousto-optical modulators (AOMs), etc.) makes it complicated and expensive to implement. Recently, fiber gratings, including long period fiber gratings (LPFGs) [11], fiber Bragg gratings (FBGs) [12] and super-structured fiber Bragg gratings (SSFBGs) [10], have been adopted as flat-top pulse shapers. The fiber grating based flat-top pulse synthesizers offer simple structure, design flexibility and inherent compatibility with fiber based communication systems. However, the fabrication of the fiber gratings involves lasers, phase masks, bulky optical systems and stringent photolithographic procedures, increasing the overall cost.

Abrupt fiber taper interferometers have previously been proposed and used as refractive-index sensors [15], [16]. An abrupt fiber taper interferometer is realized by simply concatenating two single-mode fiber tapers with a middle section of stripped single-mode fiber in between [15]. The abrupt fiber tapers, like LPFGs, couple power from the fundamental mode into cladding modes. In abrupt fiber taper interferometers, the optical power in the fundamental core mode is coupled into a series of cladding modes as it propagates along the first taper. The stripped middle section then acts as a phase shifter for different modes with negligible attenuation [15]. Finally, after the second taper, a portion of the power of the cladding modes is coupled back into the core mode. Recently, we demonstrated that flat-top pulses can be generated using an abrupt taper based MachZehnder interferometer [17]. We showed that by carefully designing the tapers and the length of the middle section, the abrupt fiber taper interferometer can be used as a flat-top pulse shaper. The fiber taper interferometer based flat-top pulse shaper offers distinct advantage over the fiber grating based counterparts: unlike fiber gratings, only a fusion splicer is needed in the fabrication of the abrupt fiber taper interferometers, making it easy and cheap to implement. In this paper, we investigate in detail the picosecond and sub-picosecond flat-top pulse generation using this abrupt taper interferometer. We first derive the theoretical model of the abrupt fiber taper interferometers based on coupled mode equations. We then simulate the pulse propagation along different abrupt fiber taper interferometers to get an optimum flat-top pulse output. Finally, we demonstrate that a 3.8-ps flat-top pulse is successfully generated from a 2.2-ps Gaussian input pulse, using the fabricated abrupt fiber taper interferometer with the parameters obtained from the simulation. We find that the simulations show a good agreement with the experimental results.

II. Theory

Conventional coupled mode theory is used here to model the pulse propagation through the abrupt fiber taper interferometers

Manuscript received June 24, 2009. First published October 30, 2009; current version published March 05, 2010. This work was supported in part by the Natural Science and Engineering Council of Canada (RGPIN 311817-06).

C. Guo is with Centre for Optical and Electromagnetic Research, Joint Laboratory of Optical Communications, Zhejiang University, Hangzhou 310058, China, and also with the Department of Electrical and Computer Engineering, Queen's University, Kingston, ON K7L3N6, Canada.

M. Nix and S. Yam are with the Department of Electrical and Computer Engineering, Queen's University, Kingston, ON K7L 3N6, Canada (e-mail: scott.yam@queensu.ca).

S. He is with the Centre for Optical and Electromagnetic Research, Joint Laboratory of Optical Communications, Zhejiang University, Hangzhou 310027,China, and also with the Alfven Laboratory, Royal Institute of Technology, S-100 44 Stockholm, Sweden (e-mail: sailing@zju.edu.cn).

Digital Object Identifier 10.1109/JLT.2009.2034985

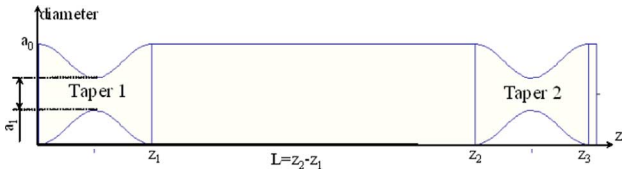

Fig. 1. Illustration of the cross-section of a typical abrupt fiber taper interferometer.

[18], [21]. The structure of a typical abrupt fiber taper interferometer is shown in Fig. 1. The taper function used in this simulation is given by

$$a(z) = \begin{cases} a_0, & \text{for } z \le 0 \text{ or } z \ge z_1 \\ a_0 - (a_0 - a_1)\sin^2\left(\pi \cdot \frac{z}{z_1}\right), & \text{for } 0 \le z \le z_1. \end{cases} \tag{1}$$

where a_0 is the fiber core diameter, a_1 is the taper waist diameter, and z_1 is the length of the taper region. Taper 1 and taper 2 shown in Fig. 1 are assumed to be the same in this simulation.

According to coupled mode theory, the propagation of the electrical field in the abrupt fiber taper is described as a combination of a series of local modes

$$\hat{\psi}(r,z) = \sum_i A_i(z)\widehat{\psi}_i(r,\beta_i(z)). \tag{2}$$

where $A_i(z)$, $\widehat{\psi}_i$, and β_i represent the amplitudes, the electrical field, and the propagation constants of the ith local mode, respectively. The coupling between the local modes is given by [18]

$$\frac{dA_i(z)}{dz} - j\beta_i(z)A_i(z) = \sum_{l\neq i} \kappa_{il}(z)A_l(z). \tag{3}$$

where the amplitude coupling coefficient can be calculated by computing the overlap integral of the ith and lth local mode

$$|\kappa_{il}(z)|^2 = \frac{|\int_A \widehat{\psi}_i^{\,*}\hat{\psi}_l dA|^2}{\int_A |\hat{\psi}_i|^2 dA \int_A |\hat{\psi}_l|^2 dA}. \tag{4}$$

$\kappa_{il}(z)$ is the coupling coefficient between the ith and lth local modes. The integration range extends over the transverse section of the waveguide at position z.

Although the coupled-mode equations are derived in the context of a continuous wave source with monochromatic wavelength, for linear pulse propagation, the response can be obtained by calculating the response of each spectral component separately and then integrating over the spectrum of the input pulse [19]. Once the spectral response $(Y(\omega))$ of the input pulse is obtained, the temporal output $(y(t))$ can be calculated using the inverse Fourier transform

$$y(t) = \frac{1}{2\pi}\int Y(\omega)e^{j\omega t}d\omega. \tag{5}$$

The general solutions of (3) can be rewritten in the form of a transmission matrix as [20]

$$\begin{pmatrix} A_1(z,f) \\ \vdots \\ A_i(z,f) \\ \vdots \\ A_n(z,f) \end{pmatrix} = \begin{bmatrix} T_{11}(z,f) & \cdots & T_{1j}(z,f) & \cdots & T_{1m}(z,f) \\ \vdots & \vdots & \vdots & \vdots & \vdots \\ T_{i1}(z,f) & \cdots & T_{ij}(z,f) & \cdots & T_{im}(z,f) \\ \vdots & \vdots & \vdots & \vdots & \vdots \\ T_{n1}(z,f) & \cdots & T_{\mathrm{nj}}(z,f) & \cdots & T_{nm}(z,f) \end{bmatrix} \times \begin{pmatrix} A_1(0,f) \\ \vdots \\ A_j(0,f) \\ \vdots \\ A_m(0,f) \end{pmatrix} \tag{6}$$

where $A_j(0,f)$ is the input amplitude at the coordinate $z = 0$, $A_i(z,f)$ is the output amplitude, and $T_{ij}(z,f)$ is the transfer function. The coefficient m and n represent the numbers of input and output modes, respectively.

In the fiber tapers the coupling occurs between modes of the same symmetry [20], e.g., LP_{01} mode only couples with LP_{0m} modes. When the single mode fiber based abrupt taper interferometer is considered, only the fundamental core mode (LP_{01}) is excited by the pulse launched into the pulse shaper (see Fig. 1). Assuming that the amplitude of the input LP_{01} mode $(A_1(0,f))$ is normalized to unity. The transmission matrix at $z = z_1$ can be expressed as

$$T_{i1}(z_1,f) = \kappa_{i1}(z_1) = |\kappa_{i1}(z_1)|e^{j\phi_{i1}} \tag{7}$$

Equations (2) and (6) can then be rewritten as

$$\begin{aligned} \widehat{\psi}(r,z_1) &= \sum_{i=1}^{n} A_i(z_1,f)\widehat{\psi}_i(r,\beta_i(z_1)) \\ &= \sum_{i=1}^{n} T_{i1}(z_1,f)A_1(0,f)\widehat{\psi}_i(r,\beta_i(z_1)) \\ &= \sum_{i=1}^{n} |\kappa_{i1}(z_1)|e^{j\phi_{i1}}\widehat{\psi}_i(r,\beta_i(z_1)). \end{aligned} \tag{8}$$

where $|\kappa_{i1}(z_1)|$ is the amplitude coupling coefficient between LP_{0i} mode and LP_{01} mode, ϕ_{i1} is the phase delay of LP_{0i} mode with respect to LP_{01} mode, and n is the number of modes excited after taper 1 (see Fig. 1). These modes then undergo different phase shifts after propagating through the stripped middle section with negligible attenuation. Although n local modes are excited by taper 1, only the fundamental core mode (LP_{01}) can be transmitted in the single mode fiber after taper 2. Therefore, only the LP_{01} mode and its corresponding transfer function $A_1(z_3,f)$ should be considered at the output $(z = z_3)$.

Assuming that the coupling between LP_{01} mode and the LP_{0i} mode is symmetric, i.e., $T_{i1}(z,f) = T_{1i}(z,f), \phi_{i1} = -\phi_{1i}$, and the two fiber tapers shown in Fig. 1 are identical so that $|\kappa_{i1}(z_1,f)| = |\kappa_{1i}(z_3,f)|$. The output after the second taper can then be obtained from (2), (7) and (8) (note that $A_1(0,f)$ is normalized to unity.)

$$A_1(z_3,f) = A_1(0,f)\sum_{i=1}^{n} T_{1i}(z_1,f)^2 e^{j(\phi_{i1}+\phi_{1i}+\phi_i)} = \sum_{i=1}^{n} |\kappa_{i1}(z_1,f)|^2 e^{j\phi_i(f)}. \quad (9)$$

where

$$|\kappa_{i1}(z_1,f)|^2 = \frac{|\int_A \hat{\psi}_{0i}^* \hat{\psi}(z_1) dA|^2}{\int_A |\hat{\psi}_{0i}|^2 dA \int_A |\hat{\psi}(z_1)|^2 dA}. \quad (10)$$

$$\phi_i(f) = \frac{\frac{2\pi}{c}[f n_{\text{eff}}(f) - f_0 n_{\text{eff}}(f_0)]}{2\pi(f-f_0)} Lf = \tau_i L f \quad (11)$$

$\hat{\psi}_{0i}^*$ is the conjugate of the modal field of LP_{0i}, $\hat{\psi}(z_1)$ is the electrical field when $z = z_1$ (see Fig. 1), ϕ_i is the phase shift of LP_{0i} mode after propagating through the middle section, f_0 is the center frequency, $n_{\text{eff}}(f)$ and $n_{\text{eff}}(f_0)$ are the effective refractive indices at frequency f and f_0, respectively, τ_i is the group delay of LP_{0i}, and L is the length of the middle section. Using (9)–(11), the response at spectral component f can be obtained. The spectral response of the abrupt fiber taper interferometer can then be calculated by integrating the response over the spectrum of the input pulse. Assuming that the temporal input pulse is $x(t)$, the temporal response can thus be calculated by

$$y(t) = \int X(f) \left[\sum_{i=1}^{n} \kappa_i^2(z_1,f) e^{j\phi_i(f)}\right] e^{j2\pi f t} df. \quad (12)$$

where $X(f)$ is the Fourier transform of the input pulse $x(t)$. Note that since only coupling between LP_{01} and LP_{0i} mode is considered, κ_i is used instead of κ_{il} afterwards.

III. Simulations

The output electrical field $\hat{\psi}_{(z=z_2)}$, the modal field $\hat{\psi}_{0i}$, the modal index n_{0i}, and the power overlap integral k_i^2 are solved using a commercial software of OptiBPM v9.0. The following values are used for various parameters: $a_0 = 125$ (μm), $\lambda = 1.5585$ (μm), $z_1 = 700$ (μm), $n_{\text{core}} = 1.4522$, and $n_{\text{cladding}} = 1.45$. The ratio of the core radius and the cladding radius is assumed to remain unchanged along the taper. The waist diameter of the taper is tuned from 16 um to 50 um to get a set of different coupling coefficients κ_i, and thus different spectral responses. Fig. 2(a) shows the power overlap integral of the LP_{01} mode and the output field ($|\kappa_1|^2$) versus the taper waist diameter a_1 at $z_1 = 700$ μm (after the first taper shown in Fig. 1). Three cases, A, B and C with respective waist diameters of 27 μm, 40 μm, and 50 μm, are chosen to calculate the spectral response, since their LP_{01} power overlap integrals after taper 1 (see Fig. 1) go from the smallest to the largest. Fig. 2(b) shows the overall local-mode power after taper 1 with respect to the input power.

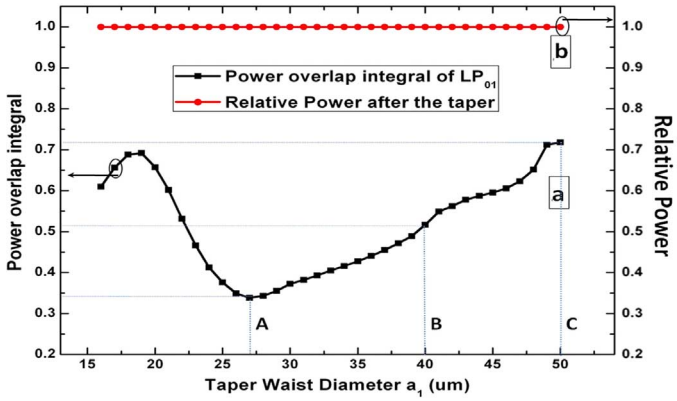

Fig. 2. (a) Power overlap integral of LP_{01} after the first taper of Fig. 1. (b) Overall local-mode power after the first taper of Fig. 1. The taper waist diameters in cases A, B, C are 27 μm, 40 μm, and 50 μm, respectively.

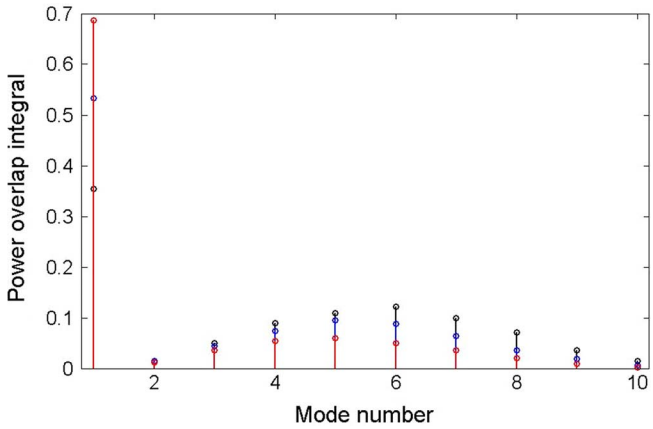

Fig. 3. The power overlap integrals of the first ten local modes ($|\kappa_1|^2 \sim |\kappa_{10}|^2$) of cases A, B, and C.

As can be seen, the radiation from the cladding is negligible, indicating that the coupled mode equations with only local modes are valid [22].

Fig. 3 shows the power overlap integrals of the first ten local modes ($|\kappa_1|^2 \sim |\kappa_{10}|^2$) of cases A, B, and C. The overall power of the first ten modes is about 98% of the incident power. Therefore, we only consider these ten modes from now on. Figs. 5 and 7 show the temporal responses and their corresponding spectral responses of the interferometers to a transform-limited Gaussian input pulse shown in Fig. 4. The full width at half-maximum (FWHM) of the Gaussian pulse is 2.2 ps, which is chosen to match the experimental conditions. The center wavelength of the Gaussian pulse is around 1.56 μm. The plots shown below are calculated using the equations discussed in Section 2. In both Fig. 5 and Fig. 7, calculation is conducted for three different waist diameters (A, B, and C). In Fig. 5, the length of the middle section (L) is set to 205 mm in all the three cases, while in Fig. 7, the length is set to 345 mm. In case B of Fig. 5, a nearly flat-top pulse with a FWHM of 4.2-ps was obtained, and the corresponding spectrum of that pulse is a sinc-like profile. In Fig. 6, this nearly flat-top pulse generation was further investigated by tuning the FWHM of the input Gaussian pulses from 2.2 ps to 3.0 ps. We found that the ripple of the output pulses deceased further when the FWHM of the input Gaussian pulses increased.

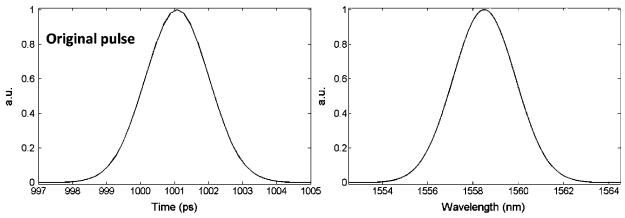

Fig. 4. Input Gaussian pulse (left) and its spectrum (right).

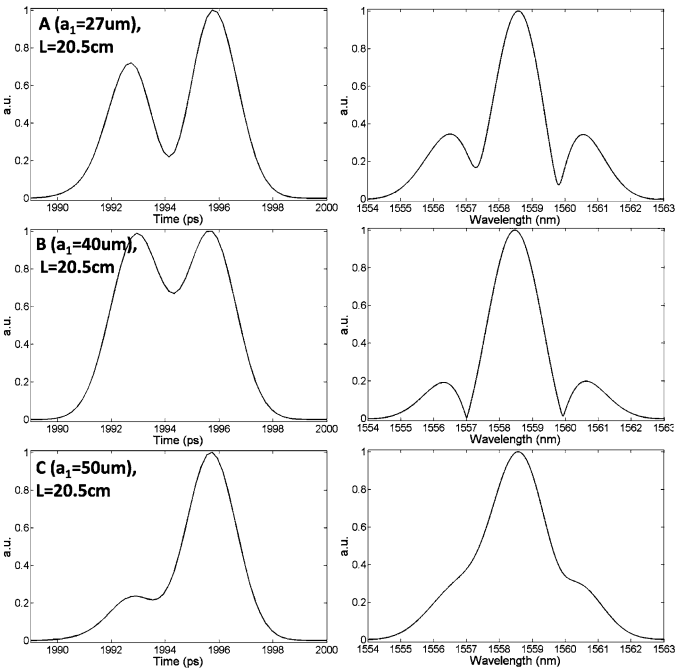

Fig. 5. Temporal responses (left) and their corresponding spectral responses (right) when the length of middle section $\mathrm{L} = 205$ mm. Three different taper waist diameters (25 μm, 40 μm, and 50 μm) are considered.

A flat-top pulse with less than 1% ripple was observed when the FWHM of the input pulse was tuned to 3.0 ps. In case B of Fig. 7, two consecutive symmetric pulses were calculated, showing the potential of the application of pulse rate multiplication using this taper based interferometer. Note that the simulated power of the temporal pulses and spectrums shown in Fig. 4–7 are represented in normalized units.

IV. Fabrication of the Abrupt Fiber Taper Interferometers and Experimental Results

As indicated in Section 3, a flat top pulse can be generated when the waist diameter of both tapers is 40 μm. The relative power of the fundamental core mode after that taper is around 50% (Fig. 2), i.e., the attenuation of the fundamental core mode power is almost 3 dB. To produce these abrupt tapers, an Ericsson FSU 995 FA fusion splicer was used to heat and draw a piece of stripped single mode fiber (SMF28) until the insertion loss measured reached 3 dB. The length of the middle section of the abrupt taper interferometer, as the simulation indicated, should be around 205 mm in order to get the appropriate spectral response necessary for synthesizing the 2.2-ps Gaussian pulse. The chemical coating along that length was removed such that there was negligible attenuation of the modes excited in the fiber

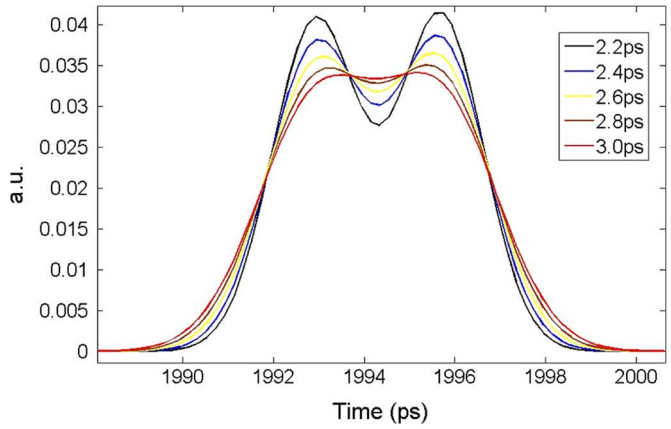

Fig. 6. Flat-top pulses with different ripples generated when the FWHM of the Gaussian input pulses is tuned from 2.2 ps to 3.0 ps.

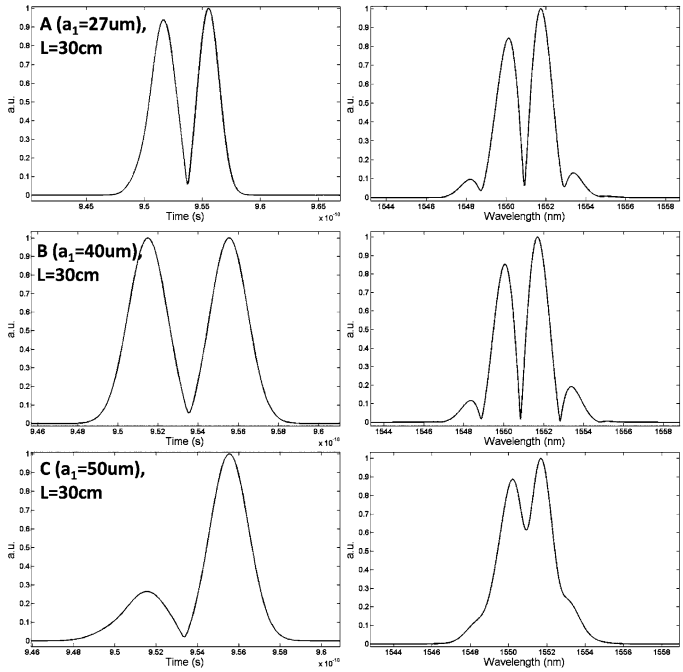

Fig. 7. Temporal responses (left) and their corresponding spectral responses (right) when the length of middle section $\mathrm{L} = 345$ mm. Three different taper waist diameters (25 μm, 40 μm, and 50 μm) are considered.

cladding. The measured length of the fabricated taper region $z_1 = 700 \pm 5$ (μm), and the measured waist diameter $a_0 = 40 \pm 2$ (μm). The measured length of the middle section of the fabricated interferometer is 204 mm. The transmission spectrum and the group delay of the fabricated interferometer measured using a Luna Optical Vector Analyzer are depicted in Fig. 8(a) and (b), respectively.

To evaluate the performance of the fabricated interferometer, an optical pulse train with a repetition rate of 9.95328 GHz, center wavelength of 1560 nm and 2.2-ps wide pulses was generated by a mode-locked fiber laser. An EDFA was applied to amplify the output pulse before it was sent to an Agilent Ultra-Wide Bandwidth Sampling Scope with an 800-GHz bandwidth. The measured input and output pulses are shown in Fig. 9(a). As one can see, a flat-top pulse was generated using the abrupt taper interferometer. The measured output flat-top pulse had a

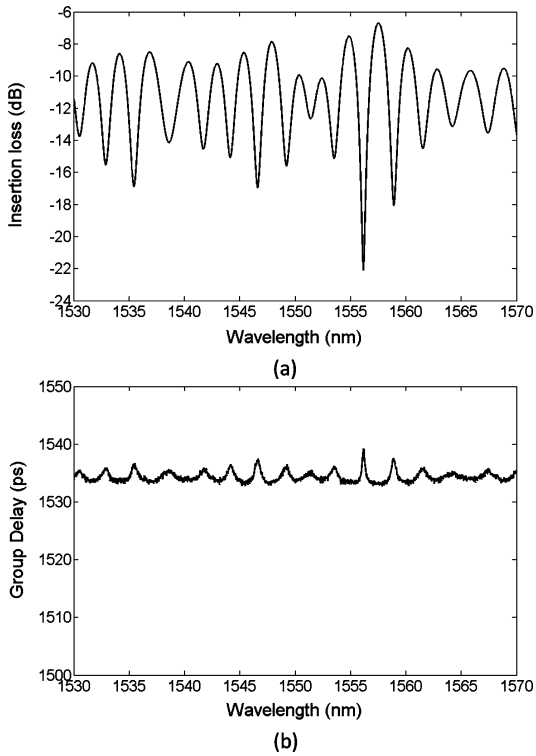

Fig. 8. (a) Transmission spectrum and (b) group delay of the fabricated interferometer.

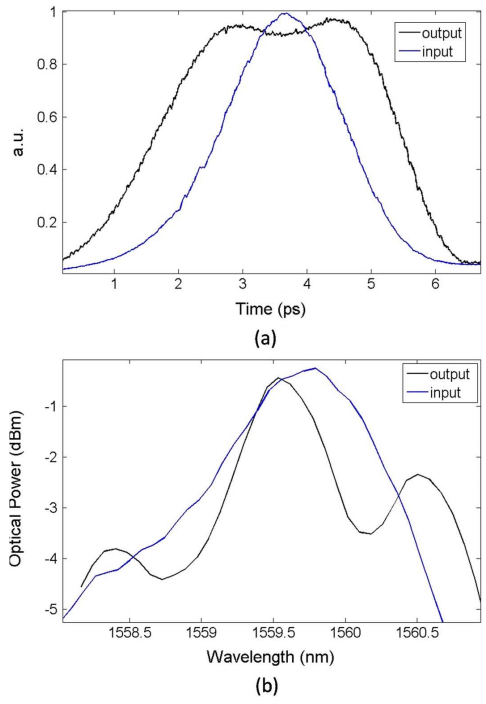

Fig. 9. (a) Input (blue) and output (black) pulses measured with an Agilent Ultra Wideband Sampling Scope. (b) Their spectrums.

FWHM of about 3.8 ps with a ripple of less than 4%. The spectra envelope of the input and output pulse were also measured and are shown in Fig. 9(b). For the sake of clarity, the modes of the laser are suppressed and only the spectral envelope is shown. As can be seen, the output spectrum does show a sinc-like spectrum profile. Comparing the simulation (shown in Fig. 5(B)) and experimental results (Fig. 9(a)), one can see that there is a discrepancy in the pulse width and the ripple of the output pulse between experiment and simulation. The cause of that discrepancy is as follows: (1) The input pulse used in the simulation is transform limited, while that used in the experiment is not, as shown in Fig. 9(b); (2) The group delay used in the simulation is assumed to be the same along different wavelengths, while the measured group delay shows a small fluctuation, as shown in Fig. 8(b); (3) The parameters of the fabricated interferometer do not strictly comply with that indicted in the simulation due to precision restrictions of the fusion splicer, as the fabrication of this abrupt taper interferometer requires precise control of the length, the diameter and the profile of the tapers.

Although the pulse widths used in the simulation and experiment are in the picosecond regime, one can easily apply this technique to sub-picosecond pulse applications. For synthesizing flat-top pulses of smaller pulse widths, the transmission nulls shown in Fig. 8(a) should be farther apart. This can be easily done by decreasing the length (L) of the middle section of the interferometer, as is indicated by (11).

V. Conclusion

In this paper, we have proposed and investigated in detail a novel and inexpensive method for synthesizing flat-top pulses in the picosecond and sub-picosecond regime. This technique is based on reshaping a Gaussian-like input pulse using a properly designed abrupt taper interferometer. We have simulated the picosecond pulse propagation through the abrupt taper interferometer based on coupled mode equations to obtain the parameters used for the fabrication. The fabricated interferometer is capable of producing a 3.8-ps flat-top pulse with less than 4% ripple from a 2.2-ps Gaussian-like input pulse. The proposed technique is easy and cheap to implement, since only a fusion splicer is needed to fabricate the interferometers. Although the pulse widths used in the simulation and experiment are a few picoseconds, this technique can be easily applied in the sub-picosecond regime by decreasing the length of the middle section of the interferometer.

Acknowledgment

The authors would like to acknowledge CMC Microsystems (www.cmc.ca) for providing access to simulation software OptiBPM v9.0 and experimental assistance. Some measurements were made with equipment from the National Microelectronics and Photonics Testing Collaboratory.

References

[1] A. M. Weiner, Y. Silberberg, H. Fouckhardt, D. E. Leaird, M. A. Saifi, M. J. Andrejco, and P. W. Smith, "Use of femtosecond square pulses to avoid pulse breakup in all-optical switching," *IEEE J. Quantum Electron.*, vol. 25, no. 12, pp. 2648–2655, Dec. 1989.

[2] T. Morioka, S. Kawanishi, H. Takara, and M. Saruwatari, "Multiple-output, 100 Gbit/s all-optical demultiplexer based on multichannel four-wave mixing pumped by a linearly-chirped square pulse," *Electron. Lett.*, vol. 30, no. 23, pp. 1959–1960, Nov. 1994.

[3] J. H. Lee, L. K. Oxenlwe, M. Ibsen, K. S. Berg, A. T. Clausen, D. J. Richardson, and P. Jeppesen, "All-optical TDM data demultiplexing at 80 Gb/s with significant timing jitter tolerance using a fiber Bragg grating based rectangular pulse switching technology," *J. Lightw, Technol.*, vol. 21, no. 11, pp. 2518–2523, Nov. 2003.

[4] T. Hirooka, K.-I. Hagiuda, T. Kumakura, K. Osawa, and M. Nakazawa, "160-Gb/s–600-km OTDM transmission using time-domain optical fourier transformation," *IEEE Photon. Technol. Lett.*, vol. 18, no. 24, pp. 2647–2649, Dec. 2006.

[5] R. Slavik, L. K. Oxenlowe, M. Galili, H. C. H. Mulvad, Y. Park, J. Azana, and P. Jeppesen, "Demultiplexing of 320-Gb/s OTDM data using ultrashort flat-top pulses," *IEEE Photon. Technol. Lett.*, vol. 19, no. 22, pp. 1855–1857, Nov. 2007.

[6] L. K. Oxenløwe, R. Slavík, M. Galili, H. C. H. Mulvad, Y. Park, J. Azaña, and P. Jeppesen, "Flat-top pulse enabling 640 Gb/s OTDM demultiplexing," in *Proc. CLEO/Europe IQEC 2007 Conf. Digest*, 2007, paper CI8_1.

[7] A. M. Weiner, J. P. Heritage, and R. N. Thurston, "Synthesis of phase-coherent, picosecond optical square pulses," *Opt. Lett.*, vol. 11, no. 3, pp. 153–155, Mar. 1986.

[8] A. M. Weiner, "Femtosecond pulse shaping using spatial light modulators," *Rev. Sci. Instrum.*, vol. 71, no. 5, pp. 1929–1960, May 2000.

[9] M. R. Fetterman, D. Goswami, D. Keusters, W. Yang, J.-K. Rhee, and W. S. Warren, "Ultrafast pulse shaping: Amplification and characterization," *Opt. Exp.*, vol. 3, no. 10, pp. 366–375, Nov. 1998.

[10] P. Petropoulos, M. Ibsen, A. D. Ellis, and D. J. Richardson, "Rectangular pulse generation based on pulse reshaping using a superstructured fiber Bragg grating," *J. Lightw. Technol.*, vol. 19, no. 5, pp. 746–752, May 2001.

[11] Y. Park, M. Kulishov, R. Slavík, and J. Azaña, "Picosecond and sub-picosecond flat-top pulse generation using uniform long-period fiber gratings," *Opt. Exp.*, vol. 14, no. 25, pp. 12670–12678, Dec. 2006.

[12] M. A. Preciado and M. A. Muriel, "Flat-top pulse generation based on a fiber bragg grating in transmission," *Opt. Lett.*, vol. 34, no. 6, pp. 752–754, Mar. 2009.

[13] W.-L.-J. Hasi, Z.-W. Lu, S.-J. Liu, Q. Li, G.-H. Yin, and W.-M. He, "Generation of flat-top waveform in the time domain based on stimulated Brillouin scattering," *Appl. Phys. B: Lasers Optics*, vol. 90, no. 3, pp. 503–506, Mar. 2008.

[14] Y. Park, M. H. Asghari, T.-J. Ahn, and J. Azaña, "Transform-limited picosecond pulse shaping based on temporal coherence synthesization," *Opt. Exp.*, vol. 15, no. 15, pp. 9584–9599, July 2007.

[15] Z. Tian, S. Yam, J. Barnes, W. Bock, P. Greig, J. Fraser, H. Loock, and R. Oleschuk, "Refractive index sensing with Mach Zehnder interferometer based on concatenating two single mode fiber tapers," *IEEE Photon. Technol. Lett.*, vol. 20, no. 8, pp. 626–628, Apr. 2008.

[16] Z. Tian, S. Yam, and H. Loock, "Refractive index sensor based on an abrupt taper Michelson interferometer in a single mode fiber," *Opt. Lett.*, vol. 33, no. 10, pp. 1105–1107, May 2008.

[17] M. Nix and S. Yam, "Flat-top pulse generation using 3-dB abrupt taper interferometeric pulse shaper," in *Proc. Optical Fiber Commun. Conf. 2009, OSA Tech. Digest*, 2009, paper OWN2.

[18] A. W. Snyder and J. D. Love, *Optical Waveguide Theory*. London, U.K.: Chapman and Hall, 1995.

[19] L. R. Chen, S. D. Benjamin, P. W. E. Smith, and J. E. Sipe, "Ultrashort pulse reflection from fiber gratings: A numerical investigation," *J. Lightw. Technol.*, vol. 15, no. 8, pp. 1503–1512, Aug. 1997.

[20] M. Kulishov and J. Azaña, "Ultrashort pulse propagation in uniform and nonuniform waveguide long-period gratings," *J. Opt. Soc. Amer. A*, vol. 22, no. 7, pp. 1319–1333, July 2005.

[21] F. Gonthier, A. Hénault, S. Lacroix, R. J. Black, and J. Bures, "Mode coupling in nonuniform fibers: Comparison between coupled-mode theory and finite-difference beam-propagation method simulations," *J. Opt. Soc. Amer. B*, vol. 8, no. 2, pp. 416–421, Feb. 1991.

[22] S. Lacroix, R. Bourbonnais, F. Gonthier, and J. Bures, "Tapered monomode optical fibers: Understanding large power transfer," *Appl. Opt.*, vol. 25, no. 23, pp. 4421–4425, Dec. 1986.

Changjian Guo (S'09) received the B.S. degree in measurement and control technology and instrumentation in 2006 from Dalian University of Technology, China. Since 2006, He has been working towards the Ph.D. degree in Zhejiang University, Hangzhou, China.

His research interests include fiber optical communication and networking.

Michael Nix received the B.Sc.Eng. degree in electrical engineering from Queen's University at Kingston, ON, Canada, where he is currently working towards the M.Sc.Eng. degree.

His research interests include multimode fiber communications systems and their impairments.

Scott S.-H. Yam (S'00–M'04) received the B.Eng. degree from the University of Waterloo, Waterloo, ON, Canada, in 1998, and the M.Sc. and Ph.D. degrees from Stanford University, Stanford, CA, in 2000, 2004, respectively.

From 2000 to 2003, he worked as a Sprint Fellow at the Sprint Advanced Technology Laboratories (ATL) in Burlingame, California. He is currently working as an assistant professor in Queen's University, Kingston, ON, Canada, researching on data transmission over multimode optical fiber and optical sensors. He has more than 50 technical journal and conference publications, as well as 2 patents and 1 pending patent application.

Dr. Yam has also served as a reviewer for the IEEE/OSA JOURNAL OF LIGHTWAVE TECHNOLOGY (JLT), IEEE JOURNAL OF SELECTED TOPICS IN QUANTUM ELECTRONICS (JSTQE), IEEE PHOTONICS TECHNOLOGIES LETTERS (PTL), *Electronics Letters, Journal of Optics A (*JOPA), and *Optics Communications*. He is a recipient of the Young Scientist Award in 2003, and Student Paper Award in 2002, both from the IEEE LEOS Japan Chapter. He is currently the past chair of the IEEE Kingston Section. He is a member of the IEEE Laser and Electro-optics Society, the IEEE Communications Society, and the Optical Society of America (OSA).

Sailing He (M'92–SM'98) received the Licentiate of Technology and Ph.D. degrees in electromagnetic theory from the Royal Institute of Stockholm, Sweden, in 1991 and 1992, respectively.

After the Ph.D. degree, he has worked at the KTH (Royal Institute of Technology), Stockholm, Sweden, as an Assistant Professor, an Associate Professor, and a Full Professor. He has also been with Zhejiang University, Hangzhou, China, since 1999 when appointed as a "Chang-Jiang project" Professor by the Ministry of Education of China. He is a Chief Scientist for JORCEP (the Joint Research Center of Photonics of KTH and Zhejiang University). He has first-authored one monograph (Oxford University Press) and authored/coauthored about 300 papers in refereed international journals.

Dr. He is a Fellow of the Optical Society of America (OSA).